

Discrepant electrophysiological characteristics and calcium homeostasis of left atrial anterior and posterior myocytes

Kazuyoshi Suenari · Yao-Chang Chen ·
Yu-Hsun Kao · Chen-Chuan Cheng ·
Yung-Kuo Lin · Yi-Jen Chen · Shih-Ann Chen

Received: 6 April 2010/Revised: 13 October 2010/Accepted: 22 October 2010/Published online: 12 November 2010
© Springer-Verlag 2010

Abstract The left atrial (LA) posterior wall has been demonstrated to have regional electrophysiological differences with a higher arrhythmogenic potential leading to atrial fibrillation (AF). However, the ionic characteristics and calcium regulation in the LA anterior and posterior myocytes have not been fully elucidated. The purpose of this study was to investigate the electrical characteristics of the LA anterior and posterior myocytes. Whole-cell patch-clamp techniques and the indo-1 fluorimetric ratio technique were used to investigate the characteristics of the ionic currents, action potentials, and intracellular calcium

in single isolated rabbit myocytes in the LA anterior and posterior walls. The expression of the Na^+ - Ca^{2+} exchanger (NCX) and ryanodine receptor (RyR) were evaluated by a Western blot. The LA posterior myocytes ($n = 15$) had a higher incidence (53 vs. 19%, $P < 0.05$) of delayed afterdepolarizations than the LA anterior myocytes ($n = 16$). The LA posterior myocytes had larger sodium currents and late sodium currents, but smaller inward rectifier potassium currents than the LA anterior myocytes. The LA posterior myocytes had larger intracellular Ca^{2+} transient and sarcoplasmic reticulum Ca^{2+} contents as compared with the LA anterior myocytes. However, the NCX currents in the LA posterior myocytes were smaller than those in the LA anterior myocytes. The LA posterior myocytes had a smaller protein expression of NCX, but a larger protein expression of RyR than the LA anterior myocytes. In conclusion, LA posterior myocytes contain a high arrhythmogenic potential and distinctive electrophysiological characteristics, which may contribute to the pathophysiology of AF.

K. Suenari
Department of Cardiovascular Medicine,
Hiroshima University Graduate School of Biomedical Sciences,
Hiroshima, Japan

Y.-H. Kao · Y.-K. Lin · Y.-J. Chen (✉)
Division of Cardiovascular Medicine,
Taipei Medical University-Wan Fang Hospital,
111, Hsin-Lung Road, Sec. 3, Taipei, Taiwan
e-mail: a9900112@ms15.hinet.net

Y.-H. Kao · Y.-K. Lin · Y.-J. Chen
Graduate Institute of Clinical Medicine,
Taipei Medical University, Taipei, Taiwan

K. Suenari · S.-A. Chen (✉)
Division of Cardiology and Cardiovascular Research Center,
Taipei Veterans General Hospital, 201, Sec. 2, Shih-Pai Road,
Taipei, Taiwan
e-mail: epsachen@ms41.hinet.net

Y.-C. Chen
Department of Biomedical Engineering,
National Defense Medical Center, Taipei, Taiwan

C.-C. Cheng
Division of Cardiology, Chi-Mei Medical Center,
Tainan, Taiwan

Keywords Atrial fibrillation · Myocytes · Calcium regulation · Ionic currents

Introduction

Atrial fibrillation (AF) is the most common cardiac arrhythmia in clinical practice and induces cardiac dysfunction and strokes [17, 23]. Previous studies have shown that the left atrium (LA) plays an important role in the pathophysiology of AF [20, 21]. Regional differences in the electrophysiological properties of the LA have been demonstrated to contribute to the pathophysiology of AF [15, 28, 37]. The LA posterior wall exhibited more frequent

rapid and repetitive electrical discharges than the other LA regions [28, 37]. The significantly higher incidence of ectopic beats-initiating AF from the LA posterior wall suggests the arrhythmogenic potential of the LA posterior wall [18, 28]. Wongcharoen et al. [35] had shown the differential electrical characteristics between the LA anterior and posterior wall. In addition, ouabain can induce a higher rate of atrial tachyarrhythmias in the LA posterior wall. These findings suggest an arrhythmogenic potential in the LA posterior wall.

Abnormal calcium homeostasis in atrial myocytes plays a critical role in the genesis of AF [14, 26]. Atrial fibrillation is associated with an increased incidence of spontaneous calcium sparks in human atrial myocytes [14], which can be caused by calcium overload in the sarcoplasmic reticulum (SR) or increased open probability of ryanodine receptors. Moreover, late sodium current ($I_{Na-late}$) has been proposed to play a role in the distinctive arrhythmogenic potential in atrial myocytes, and $I_{Na-late}$ inhibitors have been proposed to be atrial-selective agents for AF [22]. However, the ionic characteristics and calcium regulation in the LA anterior and posterior walls have not been fully elucidated. The purpose of this study was to investigate the electrical characteristics of the LA anterior and posterior wall myocytes.

Methods

Electrophysiological study of the LA anterior and posterior myocytes

The investigation was approved by a local ethics review board (LAC-96-0060) and conformed to the institutional *Guide for the Care and Use of Laboratory Animals* and the *Guide for the Care and Use of Laboratory Animals*. Seventy-five male rabbits (age 3 months; weight 1–2 kg) were anesthetized with an intraperitoneal injection of sodium pentobarbital (40 mg kg^{-1}). A mid-line thoracotomy was then performed and the heart and lungs were removed as described previously [6, 7, 35]. For the dissection of the LA anterior and posterior walls, the LA was opened by an incision along the mitral valve annulus, extending from the coronary sinus to the septum in a Tyrode's solution with a composition (in mM) of 137 NaCl, 5.4 KCl, 1.8 CaCl_2 , 0.5 MgCl_2 , 10 HEPES, and 11 glucose; the pH was adjusted to 7.4 by titration with NaOH, which was then replaced with Ca^{2+} -free Tyrode's solution containing 300 U/ml collagenase (Sigma, Type I) and 0.5 U/ml protease (Sigma, Type XIV). The LA was separated from the pulmonary veins at the LA–pulmonary vein junction. Tissue strips from the LA anterior and posterior walls were then dissected. The LA anterior and posterior walls were gently shaken in 5–10 ml of

Ca^{2+} -free oxygenated Tyrode's solution until single myocytes were obtained. The cells were allowed to stabilize in the bath for at least 30 min before the experiments.

A whole-cell patch-clamp was performed in single isolated myocytes using an Axopatch 1D amplifier (Axon Instruments, CA, USA) at $35 \pm 1^\circ\text{C}$ [8, 33]. Borosilicate glass electrodes (o.d., 1.8 mm) were used, with tip resistances of 3–5 $\text{M}\Omega$. Before the formation of the membrane–pipette seal, the tip potentials were zeroed in Tyrode's solution. The junction potentials between the bath and pipette solution (9 mV) were corrected for the action potential (AP) recordings. The APs were recorded in a current-clamp mode and the ionic currents in a voltage-clamp mode. A small hyperpolarizing step from a holding potential of -50 mV to a testing potential of -55 mV for 80 ms was delivered at the beginning of each experiment. The area under the capacitive currents was divided by the applied voltage step to obtain the total cell capacitance. Normally 60–80% series resistance (R_s) was electronically compensated. After the compensation, the average R_s was $0.75 \pm 0.05 \text{ M}\Omega$ ($n = 336$) with an estimated voltage error of $1.1 \pm 0.1 \text{ mV}$. The APs were elicited in cells from the LA anterior and posterior walls through brief current pulses at 1 Hz. The resting membrane potential (RMP) was measured during the period between the last repolarization and onset of the subsequent AP. The AP amplitude (APA) was obtained from the RMP to the peak of the AP depolarization. The AP duration at 90% repolarization of the amplitude was measured as the APD_{90} . A delayed afterdepolarization (DAD) was defined as the presence of a spontaneous depolarization of the impulse after full repolarization had occurred. Micropipettes were filled with a solution containing (in mM) CsCl 130, MgCl_2 1, Mg_2ATP 5, HEPES 10, EGTA 10, NaGTP 0.1, and Na_2 phosphocreatine 5, (pH of 7.2 with CsOH) for the L-type calcium current (I_{Ca-L}); containing (in mM) CsCl 133, NaCl 5, EGTA 10, Mg_2ATP 5, TEACl 20, HEPES 5 (pH 7.3 with CsOH) for the sodium current (I_{Na}); containing (in mM) 10 NaCl, 130 CsCl, 5 EGTA, 5 HEPES, 5 glucose, and 5 ATP-Mg for the $I_{Na-Late}$; containing (in mM) NaCl 20, CsCl 110, MgCl_2 0.4, CaCl_2 1.75, TEACl 20, BAPTA 5, glucose 5, Mg_2ATP 5, and HEPES 10, (pH of 7.25 with CsOH) for the Na^+ – Ca^{2+} exchanger (NCX) current; and containing (in mM) KCl 20, K aspartate 110, MgCl_2 1, Mg_2ATP 5, HEPES 10, EGTA 0.5, LiGTP 0.1, and Na_2 phosphocreatine 5, (pH of 7.2 with KOH) for the AP, and potassium currents.

The I_{Na} was recorded during depolarization from a holding potential of -120 mV to testing potentials ranging from -90 to $+60 \text{ mV}$ in 10-mV steps for 40 ms at a frequency of 3 Hz at room temperature ($25 \pm 1^\circ\text{C}$) with an external solution containing (in mM): NaCl 5, CsCl 133, MgCl_2 2, CaCl_2 1.8, nifedipine 0.002, HEPES 5 and

glucose 5 with a pH of 7.3. The $I_{Na-Late}$ was recorded at room temperature with an external solution containing (in mM): 140 NaCl, 5 CsCl, 2.0 MgCl₂, 1.8 CaCl₂, 5 HEPES, 5 glucose, and 0.002 of nicardipine. The amplitude of the $I_{Na-Late}$ at a voltage of -20 mV was measured as the mean current amplitude between 200 and 250 ms after the membrane was depolarized by a 2,000-ms pulse from -140 to -20 mV [22, 36].

The I_{Ca-L} was measured as an inward current during depolarization from a holding potential of -50 mV to testing potentials ranging from -40 to $+60$ mV in 10-mV steps for 300 ms at a frequency of 0.1 Hz by means of a ruptured patch-clamp. The NaCl and KCl in the external solution were replaced by TEACl and CsCl, respectively.

The NCX current was elicited by depolarizing pulses between -100 and $+100$ mV from a holding potential of -40 mV for 300 ms at a frequency of 0.1 Hz. The amplitudes of the NCX current were measured as 10 mM nickel-sensitive currents [33]. The external solution (in mM) consisted of NaCl 140, CaCl₂ 2, MgCl₂ 1, HEPES 5 and glucose 10 with a pH of 7.4 and contained strophanthidin (10 μ M), nitrendipine (10 μ M) and niflumic acid (100 μ M).

The transient outward potassium current (I_{to}) was studied with a double-pulse protocol. A 30-ms pre-pulse from -80 to -40 mV was used to inactivate the sodium channels, followed by a 300-ms test pulse to $+60$ mV in 10-mV steps at a frequency of 0.1 Hz. CdCl₂ (200 μ M) was added to the bath solution to inhibit I_{Ca-L} . The I_{to} was measured as the difference between the peak outward current and steady state current [29]. The ultra-rapid delayed rectifier potassium current (I_{Kur}) was studied with a double-pulse protocol, consisting of a 100-ms depolarizing pre-pulse to $+40$ mV from a holding potential of -50 mV, followed by 150-ms voltage steps from -40 to $+60$ mV in 10 mV increments at room temperature to provide an adequate temporal resolution. The I_{Kur} was measured as 4-aminopyridine (1 mM) sensitive currents [3].

The inward rectifier potassium current (I_{K1}) was activated from -40 mV to test potentials ranging from -20 to -120 mV in 10-mV steps for 1 s at a frequency of 0.1 Hz under a superfusion of CdCl₂ (200 μ M) and 4-aminopyridine (2 mM) in the bath solution. The amplitudes of the I_{K1} were measured as 1 mM barium-sensitive currents. The exponential time course of activation was measured at the test potential of -120 mV.

Measurement of changes in intracellular calcium concentration

The details have been described previously [5, 8, 33]. In brief, the intracellular Ca²⁺ was recorded using a fluorimetric ratio technique (indo-1 fluorescence) in the LA

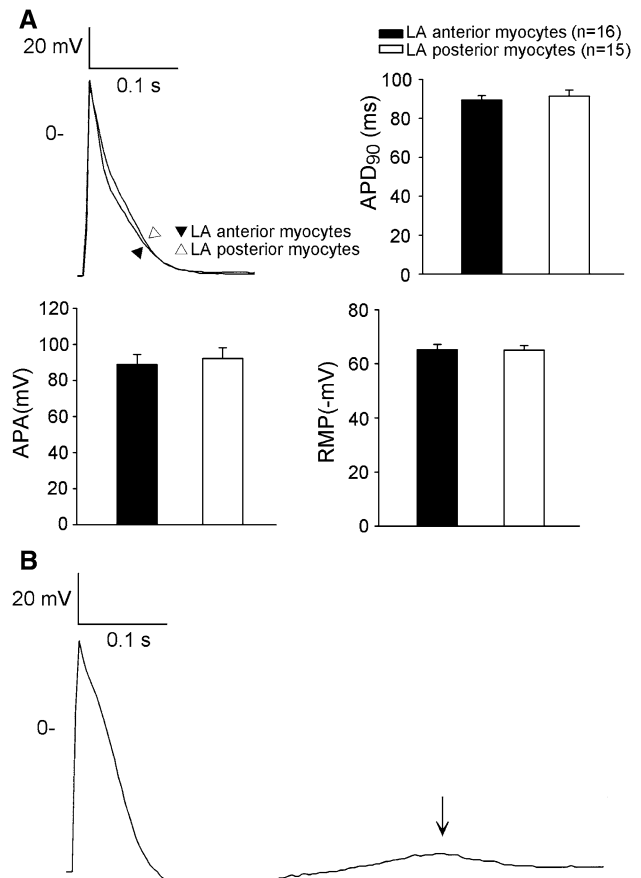


Fig. 1 **a** Action potential characteristics of the left atrial (LA) anterior and posterior myocytes. Examples and the average data of the action potentials from the LA anterior and posterior myocytes. The resting membrane potential (RMP), amplitudes of the AP (APA), and AP duration at 90% repolarization of the APA (APD₉₀) were measured at 1 Hz. **b** The delayed afterdepolarization (DAD) recorded from the LA posterior myocyte (arrow). *n* = number of myocytes

anterior and posterior myocytes. The fluorescent indicator indo-1 was loaded by incubating the myocytes at room temperature for 20–30 min with 10 μ M of indo-1/AM (Sigma Chemical, St Louis, MO, USA). The myocytes were then perfused with the Tyrode's solution at $35 \pm 1^\circ\text{C}$ for at least 20 min to wash out the extracellular indicator and to allow for the intracellular de-esterification of the indo-1. The background and cell autofluorescence were canceled out by zeroing the output of the photomultiplier tubes using cells without indo-1 loading. The experiments were performed at $35 \pm 1^\circ\text{C}$. An UV light of 360 nm with a monochromator was used for the excitation of the indo-1 from a xenon arc lamp controlled by the microfluorimetry system (OSP100-CA, Olympus, Tokyo, Japan) and the excitation light beam was directed into an inverted microscope (IX-70, Olympus). The emitted fluorescence signals from the indo-1/AM loaded myocytes were digitized at 200 Hz. The ratio of the fluorescence emission at 410 and 485 nm (R410/485) was

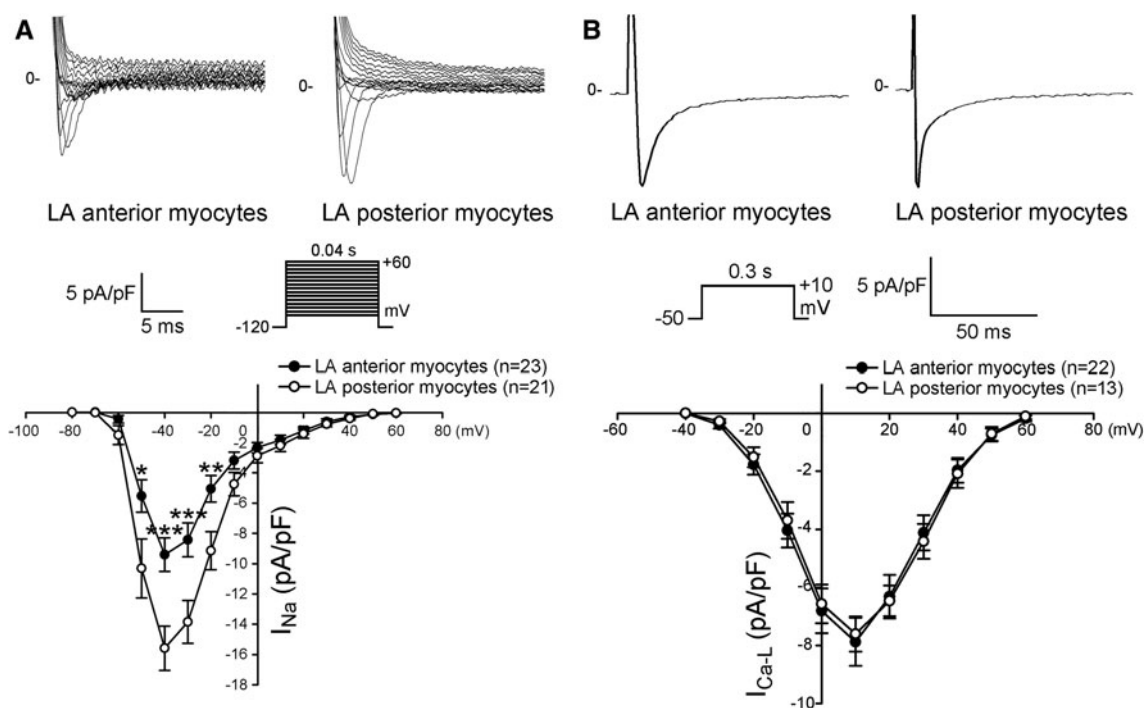
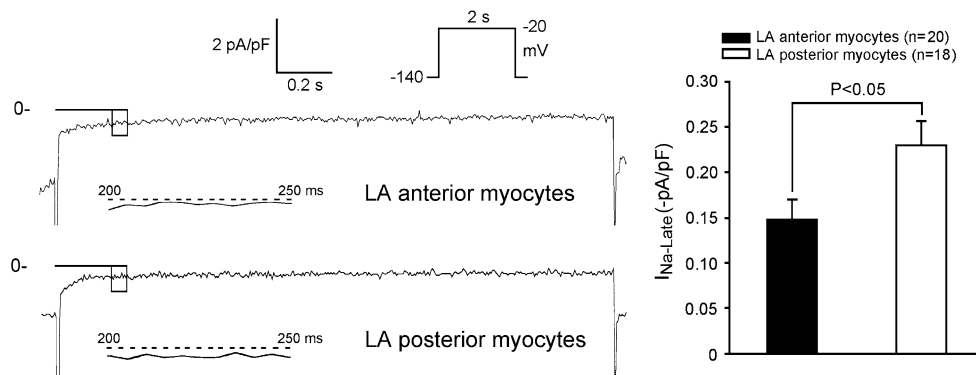


Fig. 2 The current tracing and I - V relationship of the I_{Na} and I_{Ca-L} in the LA anterior and posterior myocytes. **a** A larger I_{Na} was found in the LA posterior than in the LA anterior myocytes. **b** The I_{Ca-L} was similar

between the LA anterior and posterior myocytes. The insets in the current traces show the clamp protocol. * $P < 0.05$; ** $P < 0.01$; *** $P < 0.005$ versus LA posterior myocytes. n = number of myocytes

Fig. 3 The recordings and average data of the $I_{Na-Late}$ in the LA anterior and posterior myocytes. The bar graph shows the mean current amplitude of the $I_{Na-Late}$ in the LA anterior and posterior myocytes. The inset in the current traces shows the clamp protocol. n = number of myocytes



used as the index of the intracellular Ca^{2+} . This approach avoided any uncertainties from the calibration of the fluorescent Ca^{2+} indicators. The Ca^{2+} transient, peak systolic Ca^{2+} transient, and diastolic Ca^{2+} transient were measured during a 2 Hz field stimulation with 10 ms twice-threshold strength square-wave pulses. The Ca^{2+} transient was calculated from the difference of the peak systolic and diastolic Ca^{2+} transients. The fluorescence ratio data were processed and stored in a computer using software (OSP-SFCA, Olympus). The SR Ca^{2+} content was measured by integrating the NCX current from rapidly adding 20 mM of caffeine to the cells during rest with the membrane potential clamped to -40 mV [32]. The time integral of the NCX current was converted to amoles of Ca^{2+} released from the SR.

Western blot of the NCX and RyR protein

The myocytes from anterior and posterior LA were centrifuged and washed with cold PBS and lysed on ice for 30 min in an RIPA buffer containing 50 mM Tris, pH of 7.4, 150 mM NaCl, 1% NP40, 0.5% sodium deoxycholate, 0.1% SDS and protease inhibitor cocktails (Sigma, St Louis, MO) as described previously [5, 34]. The protein concentration was determined with a Bio-Rad protein assay reagent (Bio-Rad, Hercules, CA). Equal amounts of proteins were subjected to a sodium dodecylsulfate polyacrylamide gel electrophoresis. Blots were probed with primary antibodies against NCX (Affinity Bioreagents, Golden, CO), RyR (Affinity Bioreagents), and secondary antibodies conjugated with horse radish peroxidase. Bound antibodies were

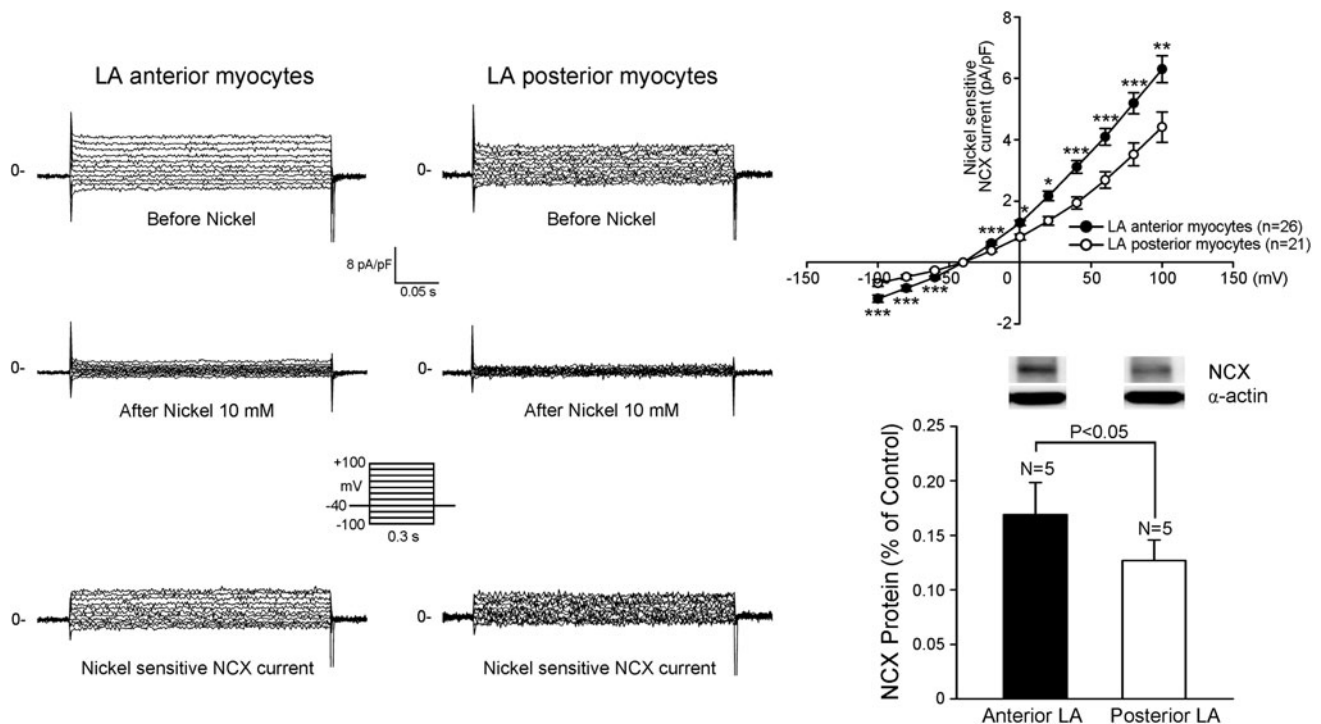


Fig. 4 The current tracings, I - V relationship of the nickel-sensitive Na^+ - Ca^{2+} exchanger (NCX) currents, and NCX protein expressions in the LA anterior and posterior myocytes. The LA posterior myocytes had significantly smaller nickel-sensitive NCX currents than the LA anterior myocytes. In addition, the posterior LA had a lesser

expression of the NCX than the anterior LA. The insets in the current traces show the various clamp protocols. * $P < 0.05$; ** $P < 0.01$; *** $P < 0.005$ versus LA posterior myocytes. n = number of myocytes, N = number of hearts

detected with the ECL detection system (Millipore, St. Louis, MO) and analyzed with Image-Pro Plus software. Targeted bands were normalized to cardiac α -sarcomeric actin (Sigma) to confirm equal protein loading.

Histology and cell morphology

The LA anterior and posterior walls were isolated from five rabbits and fixed with 4% paraformaldehyde. The specimens were sliced parallel to the wall, and stained with hematoxylin and eosin. On the histological sections, the maximum thicknesses of the LA anterior and posterior walls were measured under a light microscope (BX51, Olympus). To compare the cell morphology, isolated LA anterior and posterior myocytes were placed in an experimental chamber of a light microscope.

Statistical analysis

All quantitative data are expressed as the mean \pm SEM. An unpaired t test was used to compare the differences between the LA anterior and posterior myocytes. The nominal variables were compared by a Pearson's Chi-square test or Fisher's exact test. A P value lower than 0.05 was considered to be statistically significant.

Results

Electrophysiological characteristics of the LA anterior and posterior myocytes

The cell capacitance (49 ± 2 pF vs. 51 ± 2 pF, $P > 0.05$) was similar between the LA anterior ($n = 179$) and posterior ($n = 157$) myocytes. As shown in Fig. 1, the RMP, APA, and APD_{90} were similar for the LA anterior and posterior myocytes. However, DADs were observed in 3 of 16 LA anterior myocytes and 8 of 15 LA posterior myocytes (19 vs. 53%, $P < 0.05$). Moreover, the LA posterior myocytes tended to have larger DAD amplitudes (6.0 ± 2.2 vs. 1.4 ± 0.8 mV, $P = 0.07$) as compared with the LA anterior myocytes.

Figure 2a, b shows the tracing and I - V relationship of the I_{Na} and $I_{\text{Ca-L}}$ of the LA anterior and posterior myocytes. The current density of the peak I_{Na} in the LA posterior myocytes was significantly larger than that in the LA anterior myocytes. However, the $I_{\text{Ca-L}}$ was similar between the two groups. Moreover, the $I_{\text{Na-Late}}$ measured between 200 and 250 ms was significantly higher in the LA posterior myocytes than in the LA anterior myocytes (Fig. 3). In contrast, the LA posterior myocytes had significantly smaller nickel-sensitive NCX currents than the

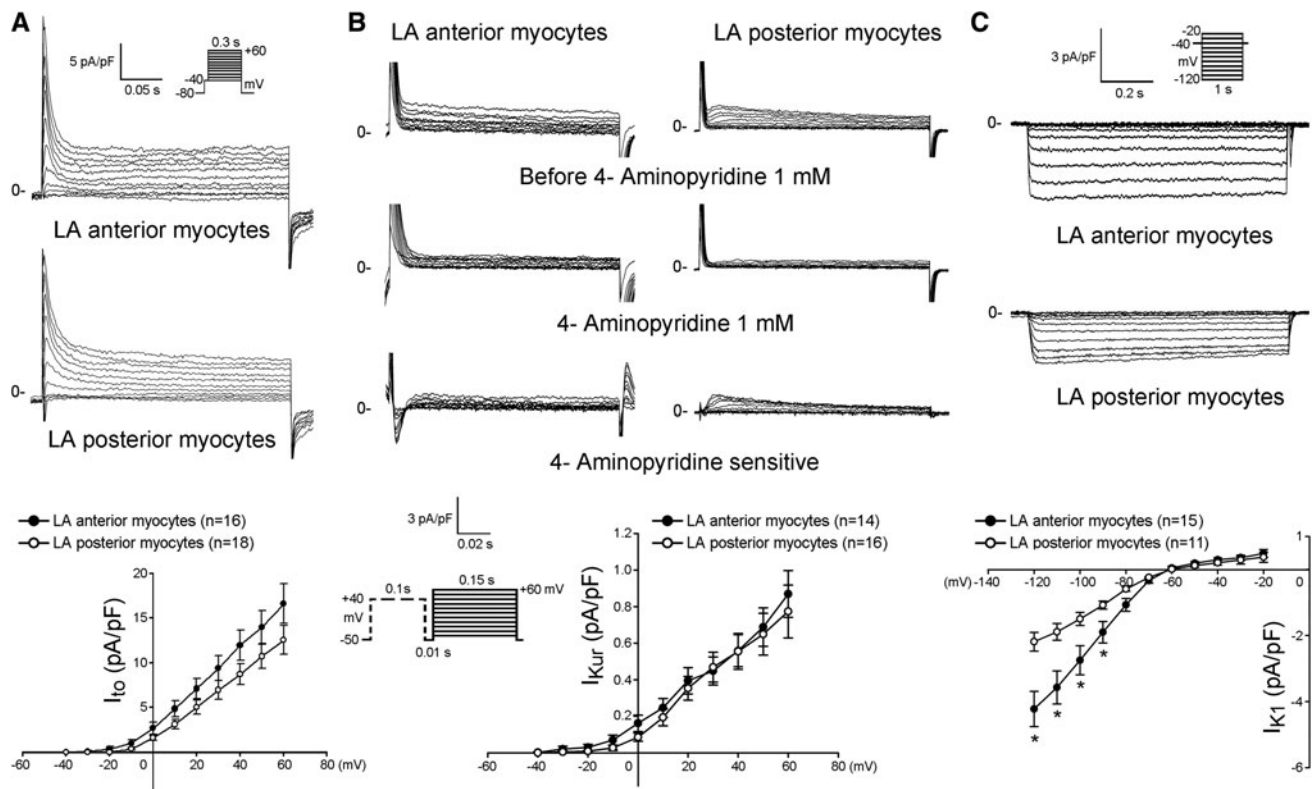


Fig. 5 The I_{to} , 4-aminopyridine-sensitive I_{Kur} , and I_{K1} in the LA anterior and posterior myocytes. **a** Examples of the tracings and I - V relationship of the I_{to} from the LA anterior and posterior myocytes. **b** Examples of the tracings and I - V relationship of the 4-aminopyridine-sensitive I_{Kur} from the LA anterior and posterior myocytes. The current amplitude of the 4-aminopyridine-sensitive

current was determined by subtracting the currents before and after wash-in of 1 mM 4-Aminopyridine. **c** Examples of the tracings and I - V relationship of the I_{K1} from the LA anterior and posterior myocytes. The insets in the current traces show the various clamp protocols. * $P < 0.05$ versus LA posterior myocytes. n = number of myocytes

LA anterior myocytes. According to the analysis of the protein level of the NCX, the LA posterior myocytes had a lesser expression of NCX than the LA anterior myocytes (Fig. 4).

Figure 5a–c shows the tracings and I - V relationship of the I_{to} , 4-aminopyridine-sensitive I_{Kur} , and I_{K1} of the LA anterior and posterior myocytes, respectively. The current densities of the I_{to} and 4-aminopyridine-sensitive I_{Kur} were similar between the LA anterior and posterior myocytes. However, the I_{K1} in the LA posterior myocytes was significantly smaller than that in the LA anterior myocytes. In addition, the activation time in the LA posterior myocytes was slower than that in the LA anterior myocytes (11.3 ± 2.9 vs. 4.9 ± 0.9 ms, $P < 0.05$).

Calcium regulation of the LA anterior and posterior myocytes

As shown in Fig. 6a, the amplitudes of the Ca^{2+} transient were larger in the LA posterior myocytes than in the LA anterior myocytes. After the rapid infusion of caffeine (20 mM), the LA posterior myocytes had larger caffeine-

induced Ca^{2+} transients, which suggested a larger SR Ca^{2+} content in the LA posterior myocytes. The integration of the caffeine-induced NCX currents further confirmed that the SR Ca^{2+} content was larger in the LA posterior myocytes than in the LA anterior myocytes (Fig. 6b). Figure 6c shows protein level of the RyR from anterior and posterior LA. Compared with the LA anterior myocytes, expression of the RyR was significantly increased in the LA posterior myocytes.

Morphology of the LA anterior and posterior wall

Figure 7a shows examples of the LA anterior and posterior walls. The maximum wall thickness (0.8 ± 0.1 vs. 1.1 ± 0.1 mm, $P < 0.05$) was thinner in the LA posterior wall ($N = 5$) than that in the LA anterior wall ($N = 5$). In addition, both the isolated LA anterior and posterior myocytes had rod-shaped morphologies (Fig. 7b). The cell length (114 ± 3 vs. 115 ± 3 μ m, $P > 0.05$) and width (13 ± 0.3 vs. 13 ± 0.4 μ m, $P > 0.05$) were similar between the LA anterior ($n = 61$) and posterior ($n = 54$) myocytes.

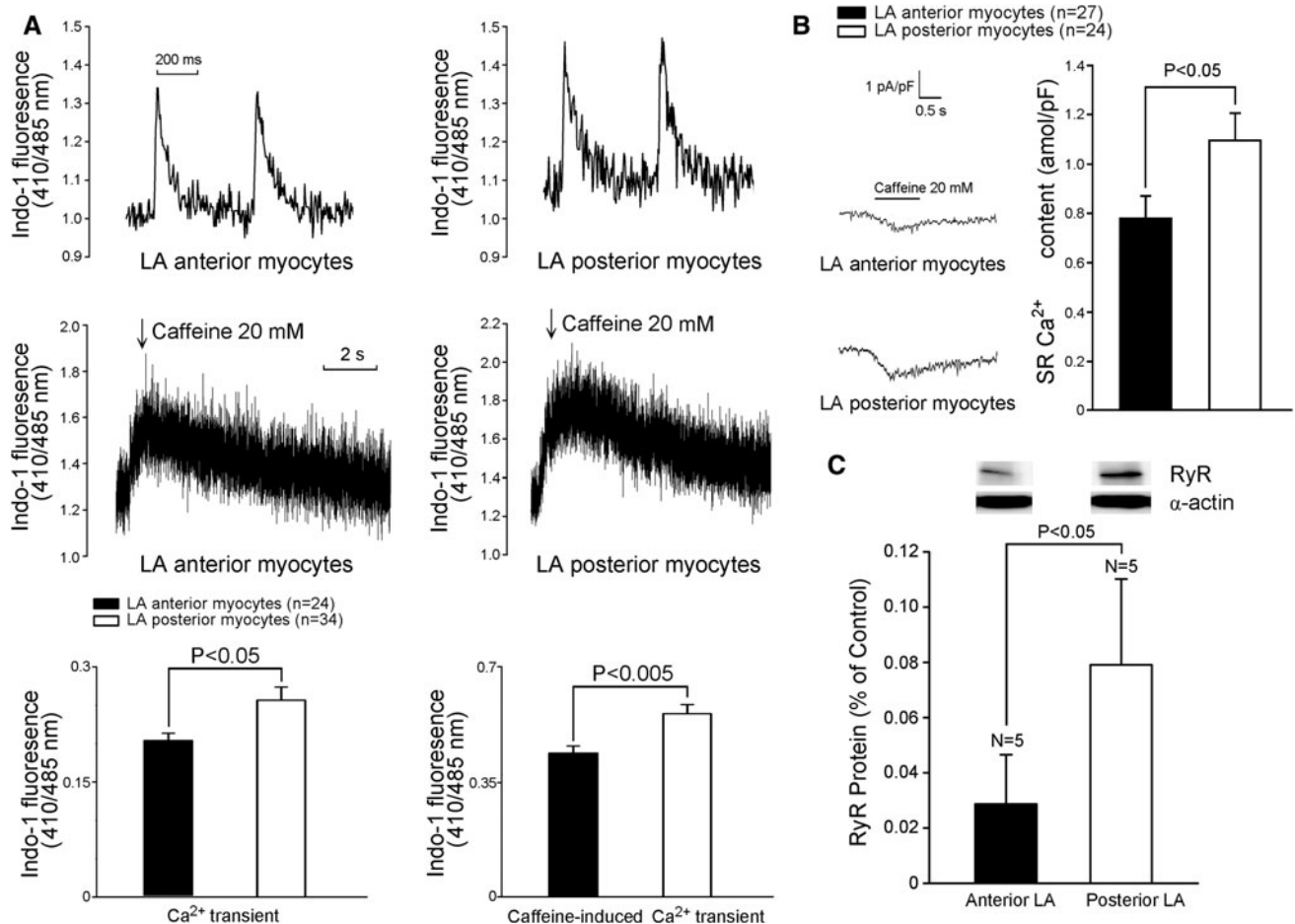


Fig. 6 The intracellular Ca²⁺ transient and Ca²⁺ stores measured from the caffeine (20 mM)-induced Ca²⁺ transient in the LA anterior and posterior myocytes. **a** The tracings and average data from the Ca²⁺ transient and caffeine-induced Ca²⁺ transients in the LA anterior and posterior myocytes. **b** The tracings and average data of the caffeine-induced Na⁺-Ca²⁺ exchanger (NCX) currents and SR

Ca²⁺ content from integrating the NCX currents in the LA anterior and posterior myocytes. **c** Expression of the ryanodine receptor (RyR) protein in the anterior and posterior LA. The posterior LA had a larger expression of the RyR than the anterior LA. *n* = number of myocytes, *N* = number of hearts

Discussion

As a significantly higher incidence of ectopic beats-initiating AF from the LA posterior wall reflected the arrhythmogenic potential of the LA posterior wall [18, 28], the present study demonstrated a higher incidence of DADs in LA posterior myocytes. Similar to that in the previous study [35], this finding confirmed the presence of a regional heterogeneous electrophysiology in the LA.

In this study, we found that the *I*_{Na} current density in the LA posterior myocytes was significantly larger than that in the LA anterior myocytes. The larger amplitude of the *I*_{Na} not only increases the intracellular Na⁺, it can also contribute to maintaining a high intracellular Ca²⁺ in the LA posterior myocytes. Additionally, the *I*_{Na-Late} in the LA posterior myocytes was significantly larger than that in the LA anterior myocytes. Previous studies have shown that the *I*_{Na-Late} plays an important role in the arrhythmogenic

potentials of the ventricles and atria [4, 12, 22, 39]. The larger *I*_{Na-Late} during the delay phase (200–250 ms) would lead to arrhythmogenesis by DADs in the LA posterior myocytes [27]. However, we also have measured the *I*_{Na-Late} at 50 ms, which was similar between LA anterior and posterior myocytes, and may play a role in the similar AP morphology in these cells. Moreover, the LA anterior and posterior myocytes have a similar *I*_{to}, 4-aminopyridine-sensitive *I*_{Kur}, and *I*_{Ca-L}, which can produce the similar AP duration in the LA anterior and posterior myocytes. Although the *I*_{K1} was smaller and slower in the LA posterior myocytes than in the LA anterior myocytes, these differences may not induce a different RMP between the LA anterior and posterior myocytes, since the different *I*_{K1} was activated by much more negative potentials than the RMP in the LA myocytes.

Whether an increased Ca²⁺ overload of the SR is arrhythmogenic or not is still controversial [31]. We found

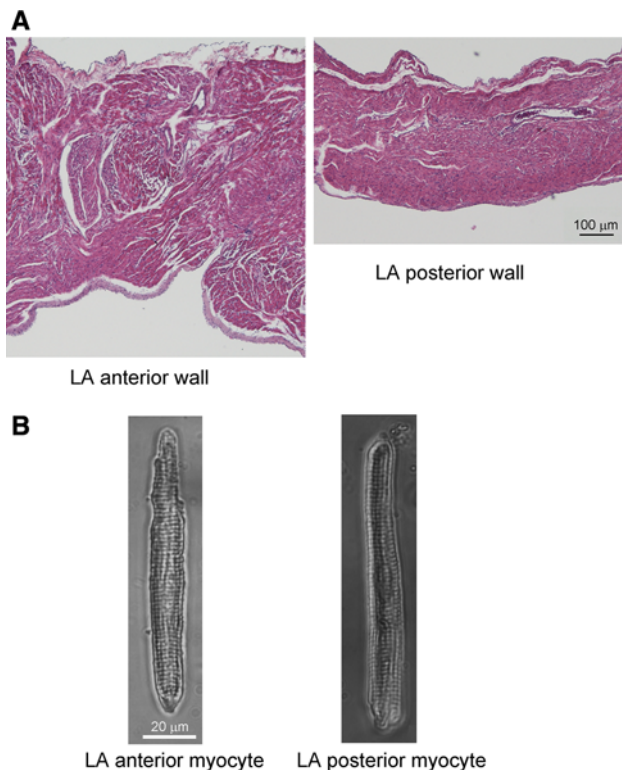


Fig. 7 Histology and cell morphology from LA anterior and posterior walls. **a** The LA poster wall was thinner than the LA anterior wall. **b** LA anterior and posterior myocytes had similar cell morphologies, cell width and length

that the LA posterior myocytes had a significantly larger Ca^{2+} transient and larger SR Ca^{2+} content than the LA anterior myocytes. The larger SR Ca^{2+} content in the LA posterior myocytes can trigger a larger Ca^{2+} transient in these cells [38]. Additionally, an increased RyR also can enhance Ca^{2+} transients. The Western blot analysis in this study showed that the LA posterior myocytes had a larger RyR expression, which may contribute to a larger Ca^{2+} transient, despite a similar $I_{\text{Ca-L}}$ between the LA anterior and posterior myocytes.

Previous studies have indicated that heart failure myocytes contain a smaller SR Ca^{2+} content and larger NCX currents, which suggest the important relationship of the NCX currents and calcium homeostasis [2, 13], because NCX plays a major role in removing the $[\text{Ca}^{2+}]_i$ as a result of decreasing the SR Ca^{2+} store [32]. In this study, we found that the LA posterior myocytes had a larger SR Ca^{2+} store and smaller NCX currents than the LA anterior myocytes, which suggests that smaller NCX currents in these cells may prevent the Ca^{2+} from being driven outside the cells to maintain the larger SR Ca^{2+} . This finding may be caused by the lesser NCX protein in the LA posterior

myocytes. Although the mechanism underlying the discrepant electrophysiological characteristics of the LA anterior and posterior myocytes were not clear, it is possible that greater stretch due to a thinner LA posterior wall may contribute to their distinctive electrophysiological characteristics [11, 25], whereas stretch can increase the intracellular Na^+ and Ca^{2+} , and result in a larger SR Ca^{2+} content and Ca^{2+} leakage which may easily trigger atrial arrhythmogenesis [1, 10, 16]. Moreover, the different embryological origins, changes in the gene expression, or post-translational modification of the proteins in the LA anterior and posterior myocytes may contribute to the regional differences in the electrophysiological findings in LA as observed in the present study [24]. However, the LA anterior and posterior myocytes had a similar cell morphology and cell size.

The present data should be interpreted with caution due to the limitations of this study. First, we investigated the differences between the LA anterior and posterior myocytes only in normal rabbits without any atrial arrhythmias. However, we demonstrated the arrhythmogenic potential of the LA posterior myocytes, therefore it is quite possible that the LA posterior wall will become arrhythmogenic during the presence of AF precipitating factors such as heart failure, dilated atria, and aging. Second, the electrophysiological characteristics of the other regions were not elucidated in this study, since we only studied the regional heterogeneity in the LA anterior and posterior myocytes. Finally, Ca^{2+} /calmodulin-dependent protein kinase II-dependent hyperphosphorylation, phospholamban phosphorylation, and local autonomic innervation play an important role in the channel regulation [9, 19, 30, 38], and the functional differences between the LA anterior and posterior myocytes require further investigation into such regulator mechanisms.

Conclusions

The present study demonstrated that regional differences in the electrophysiological properties and ionic currents existed between the LA anterior and posterior walls. The LA posterior myocytes contain a high arrhythmogenic potential due to distinctive electrophysiological characteristics, which may contribute to the pathophysiology of AF.

Acknowledgments This work was supported by the Center of Excellence for Clinical Trials and Research in Wan Fang Hospital (DOH-TD-B-111-002) and grants NSC 96-2628-B-038-012-MY3, NSC 96-2314-B-010-006, NSC 97-2314-B-038-030-MY3 and 98CM-TMU-10 from Chi-Mei Medical Center.

Conflict of interest The authors state no conflict of interest.

References

- Alvarez BV, Perez NG, Ennis IL, Camilion de Hurtado MC, Cingolani HE (1999) Mechanisms underlying the increase in force and Ca^{2+} transient that follow stretch of cardiac muscle: a possible explanation of the Anrep effect. *Circ Res* 85:716–722
- Bers DM, Eisner DA, Valdivia HH (2003) Sarcoplasmic reticulum Ca^{2+} and heart failure: roles of diastolic leak and Ca^{2+} transport. *Circ Res* 93:487–490
- Brandt MC, Priebe L, Bohle T, Sudkamp M, Beuckelmann DJ (2000) The ultrarapid and the transient outward K^{+} current in human atrial fibrillation. Their possible role in postoperative atrial fibrillation. *J Mol Cell Cardiol* 32:1885–1896
- Burashnikov A, Di Diego JM, Zygmunt AC, Belardinelli L, Antzelevitch C (2007) Atrium-selective sodium channel block as a strategy for suppression of atrial fibrillation: differences in sodium channel inactivation between atria and ventricles and the role of ranolazine. *Circulation* 116:1449–1457
- Chen YC, Kao YH, Huang CF, Cheng CC, Chen YJ, Chen SA (2010) Heat stress responses modulate calcium regulations and electrophysiological characteristics in atrial myocytes. *J Mol Cell Cardiol* 48:781–788
- Chen YC, Pan NH, Cheng CC, Higa S, Chen YJ, Chen SA (2009) Heterogeneous expression of potassium currents and pacemaker currents potentially regulates arrhythmogenesis of pulmonary vein cardiomyocytes. *J Cardiovasc Electrophysiol* 20:1039–1045
- Chen YJ, Chen YC, Tai CT, Yeh HI, Lin CI, Chen SA (2006) Angiotensin II and angiotensin II receptor blocker modulate the arrhythmogenic activity of pulmonary veins. *Br J Pharmacol* 147:12–22
- Chen YJ, Chen YC, Wongcharoen W, Lin CI, Chen SA (2008) Effect of K201, a novel antiarrhythmic drug on calcium handling and arrhythmogenic activity of pulmonary vein cardiomyocytes. *Br J Pharmacol* 153:915–925
- Chou CC, Chen PS (2009) New concepts in atrial fibrillation: neural mechanisms and calcium dynamics. *Cardiol Clin* 27:35–43, viii
- Cingolani HE, Perez NG, Pieske B, von Lewinski D, Camilion de Hurtado MC (2003) Stretch-elicited $\text{Na}^{+}/\text{H}^{+}$ exchanger activation: the autocrine/paracrine loop and its mechanical counterpart. *Cardiovasc Res* 57:953–960
- Corradi D, Callegari S, Benussi S, Maestri R, Pastori P, Nascimbene S, Bosio S, Dorigo E, Grassani C, Rusconi R, Vettori MV, Alinovi R, Astorri E, Pappone C, Alfieri O (2005) Myocyte changes and their left atrial distribution in patients with chronic atrial fibrillation related to mitral valve disease. *Hum Pathol* 36:1080–1089
- Fabritz L, Kirchhof P, Franz MR, Nuyens D, Rossenbacker T, Ottenhof A, Haverkamp W, Breithardt G, Carmeliet E, Carmeliet P (2003) Effect of pacing and mexiletine on dispersion of repolarisation and arrhythmias in DeltaKPQ SCN5A (long QT3) mice. *Cardiovasc Res* 57:1085–1093
- Hobai IA, O'Rourke B (2000) Enhanced Ca^{2+} -activated Na^{+} - Ca^{2+} exchange activity in canine pacing-induced heart failure. *Circ Res* 87:690–698
- Hove-Madsen L, Llach A, Bayes-Genis A, Roura S, Rodriguez Font E, Aris A, Cinca J (2004) Atrial fibrillation is associated with increased spontaneous calcium release from the sarcoplasmic reticulum in human atrial myocytes. *Circulation* 110:1358–1363
- Huang JL, Tai CT, Lin YJ, Ting CT, Chen YT, Chang MS, Lin FY, Lai WT, Chen SA (2006) The mechanisms of an increased dominant frequency in the left atrial posterior wall during atrial fibrillation in acute atrial dilatation. *J Cardiovasc Electrophysiol* 17:178–188
- Iribe G, Ward CW, Camelliti P, Bollensdorff C, Mason F, Burton RA, Garry A, Morphew MK, Hoenger A, Lederer WJ, Kohl P (2009) Axial stretch of rat single ventricular cardiomyocytes causes an acute and transient increase in Ca^{2+} spark rate. *Circ Res* 104:787–795
- Krahn AD, Manfreda J, Tate RB, Mathewson FA, Cuddy TE (1995) The natural history of atrial fibrillation: incidence, risk factors, and prognosis in the Manitoba follow-up study. *Am J Med* 98:476–484
- Ndrepepa G, Weber S, Karch MR, Schneider MA, Schreieck JJ, Schomig A, Schmitt C (2002) Electrophysiologic characteristics of the spontaneous onset and termination of atrial fibrillation. *Am J Cardiol* 90:1215–1220
- Neef S, Dybkova N, Sossalla S, Ort KR, Fluschnik N, Neumann K, Seipelt R, Schondube FA, Hasenfuss G, Maier LS (2010) CaMKII-dependent diastolic SR Ca^{2+} leak and elevated diastolic Ca^{2+} levels in right atrial myocardium of patients with atrial fibrillation. *Circ Res* 106:1134–1144
- Oral H, Scharf C, Chugh A, Hall B, Cheung P, Good E, Veerareddy S, Pelosi F Jr, Morady F (2003) Catheter ablation for paroxysmal atrial fibrillation: segmental pulmonary vein ostial ablation versus left atrial ablation. *Circulation* 108:2355–2360
- Pappone C, Oreto G, Rosanio S, Vicedomini G, Tocchi M, Gugliotta F, Salvati A, Dicandia C, Calabro MP, Mazzone P, Ficarra E, Di Gioia C, Gulletta S, Nardi S, Santinelli V, Benussi S, Alfieri O (2001) Atrial electroanatomic remodeling after circumferential radiofrequency pulmonary vein ablation: efficacy of an anatomic approach in a large cohort of patients with atrial fibrillation. *Circulation* 104:2539–2544
- Persson F, Andersson B, Duker G, Jacobson I, Carlsson L (2007) Functional effects of the late sodium current inhibition by AZD7009 and lidocaine in rabbit isolated atrial and ventricular tissue and Purkinje fibre. *Eur J Pharmacol* 558:133–143
- Psaty BM, Manolio TA, Kuller LH, Kronmal RA, Cushman M, Fried LP, White R, Furberg CD, Rautaharju PM (1997) Incidence of and risk factors for atrial fibrillation in older adults. *Circulation* 96:2455–2461
- Sadler TW (1990) Cardiovascular system. In: Langman J (ed) Langman's medical embryology. Williams and Wilkins, Baltimore, pp 179–227
- Saygili E, Rana OR, Meyer C, Gemein C, Andrzejewski MG, Ludwig A, Weber C, Schotten U, Kruttgen A, Weis J, Schwinger RH, Mischke K, Rassaf T, Kelm M, Schauer P (2009) The angiotensin-calcineurin-NFAT pathway mediates stretch-induced up-regulation of matrix metalloproteinases-2/-9 in atrial myocytes. *Basic Res Cardiol* 104:435–448
- Schotten U, Greiser M, Benke D, Buerkel K, Ehrenteidt B, Stellbrink C, Vazquez-Jimenez JF, Schoendube F, Hanrath P, Allessie M (2002) Atrial fibrillation-induced atrial contractile dysfunction: a tachycardiomyopathy of a different sort. *Cardiovasc Res* 53:192–201
- Song Y, Shryock JC, Belardinelli L (2008) An increase of late sodium current induces delayed afterdepolarizations and sustained triggered activity in atrial myocytes. *Am J Physiol Heart Circ Physiol* 294:H2031–H2039
- Sueda T, Nagata H, Shikata H, Orihashi K, Morita S, Sueshiro M, Okada K, Matsuura Y (1996) Simple left atrial procedure for chronic atrial fibrillation associated with mitral valve disease. *Ann Thorac Surg* 62:1796–1800
- Udyavar AR, Chen YC, Chen YJ, Cheng CC, Lin CI, Chen SA (2008) Endothelin-1 modulates the arrhythmogenic activity of pulmonary veins. *J Cardiovasc Electrophysiol* 19:285–292
- van Borren MM, Verkerk AO, Wilders R, Hajji N, Zegers JG, Bourier J, Tan HL, Verheijck EE, Peters SL, Alewijnse AE, Ravesloot JH (2010) Effects of muscarinic receptor stimulation

- on Ca^{2+} transient, cAMP production and pacemaker frequency of rabbit sinoatrial node cells. *Basic Res Cardiol* 105:73–87
31. Venetucci LA, Trafford AW, O'Neill SC, Eisner DA (2008) The sarcoplasmic reticulum and arrhythmogenic calcium release. *Cardiovasc Res* 77:285–292
 32. Walden AP, Dibb KM, Trafford AW (2009) Differences in intracellular calcium homeostasis between atrial and ventricular myocytes. *J Mol Cell Cardiol* 46:463–473
 33. Wongcharoen W, Chen YC, Chen YJ, Chang CM, Yeh HI, Lin CI, Chen SA (2006) Effects of a $\text{Na}^+/\text{Ca}^{2+}$ exchanger inhibitor on pulmonary vein electrical activity and ouabain-induced arrhythmogenicity. *Cardiovasc Res* 70:497–508
 34. Wongcharoen W, Chen YC, Chen YJ, Chen SY, Yeh HI, Lin CI, Chen SA (2007) Aging increases pulmonary veins arrhythmogenesis and susceptibility to calcium regulation agents. *Heart Rhythm* 4:1338–1349
 35. Wongcharoen W, Chen YC, Chen YJ, Lin CI, Chen SA (2007) Effects of aging and ouabain on left atrial arrhythmogenicity. *J Cardiovasc Electrophysiol* 18:526–531
 36. Wu L, Guo D, Li H, Hackett J, Yan GX, Jiao Z, Antzelevitch C, Shryock JC, Belardinelli L (2008) Role of late sodium current in modulating the proarrhythmic and antiarrhythmic effects of quinidine. *Heart Rhythm* 5:1726–1734
 37. Wu TJ, Doshi RN, Huang HL, Blanche C, Kass RM, Trento A, Cheng W, Karagueuzian HS, Peter CT, Chen PS (2002) Simultaneous biatrial computerized mapping during permanent atrial fibrillation in patients with organic heart disease. *J Cardiovasc Electrophysiol* 13:571–577
 38. Yeh YH, Wakili R, Qi XY, Chartier D, Boknik P, Kaab S, Ravens U, Coutu P, Dobrev D, Nattel S (2008) Calcium-handling abnormalities underlying atrial arrhythmogenesis and contractile dysfunction in dogs with congestive heart failure. *Circ Arrhythm Electrophysiol* 1:93–102
 39. Zellerhoff S, Pistulli R, Monnig G, Hinterseer M, Beckmann BM, Kobe J, Steinbeck G, Kaab S, Haverkamp W, Fabritz L, Gradaus R, Breithardt G, Schulze-Bahr E, Bocker D, Kirchhof P (2009) Atrial Arrhythmias in long-QT syndrome under daily life conditions: a nested case control study. *J Cardiovasc Electrophysiol* 20:401–407